Decorrelating a compressible turbulent flow: An experiment

Jason Larkin* and Walter I. Goldburg
Department of Physics & Astronomy, University of Pittsburgh, Pittsburgh, Pennsylvania 15260, USA
(Received 30 March 2010; published 1 July 2010)

Floating particles that are initially distributed uniformly on the surface of a turbulent fluid, subsequently coagulate, until finally a steady state is reached. This being so, they manifestly form a compressible system. In this experiment, the information dimension D_1, and the Lyapunov exponents of the coagulated floaters, is measured. The trajectories and the velocity fields of the particles are captured in a sequence of rapidly acquired images. Then the velocity sequence is randomly shuffled in time to generate new trajectories. This analysis mimics the Kraichnan ensemble and yields properties of a velocity correlation function that is delta correlated in time (but not in space). The measurements are compared with theoretical expectations and with simulations of Boffetta *et al.*, that closely mimic the laboratory experiment reported here.

DOI: 10.1103/PhysRevE.82.016301 PACS number(s): 47.27.ed, 47.52.+j

I. INTRODUCTION

It has become a standard procedure to study fluid flows by tracking the trajectories of small particles introduced into the flow. Assume first that the fluid is highly viscous and moves azimuthally between two concentric cylinders, one of which is rotating at constant angular velocity. A series of consecutive and rapid velocity measurements will reveal that each particle is moving in a circle. Now imagine that the series of consecutive velocity measurements is randomly rearranged, as one might shuffle a deck of cards. If the shuffled velocity field is then used to evolve tracer particles (explained in the Experiment section), they will appear to be jerking back and forth. Nonetheless, the circularity of the trajectories will be recognizable. Now imagine that the fluid is turbulent rather than laminar and that the frame rate of the camera (in Hz) is much faster than the inverse lifetime of the smallest eddies. Will the randomly shuffled sequence of measurements contain information about the turbulence, as in the laminar case?

This laboratory study was motivated by a computer simulation of this same problem by Boffetta *et al.* (to be called BDES) [1]. That simulation, in turn, was inspired by a theoretical analysis of velocity fluctuations by R. Kraichnan [2]. Concentrating on the two-point velocity autocorrelation function, Kraichnan argued that one could increase our understanding of turbulence by making the simplifying assumption that velocity fluctuations are delta correlated in time, while retaining the spatial dependence of the fluctuations. Kraichnan's approach is related to prior work of L. F. Richardson, who analyzed the time evolution of the separation of particle pairs in turbulent flows by treating their motion as Brownian-like [3].

This experiment, and the computer simulations of BDES, focuses on an unusual type of flow, namely the motion of low-density particles that float on a turbulent, three-dimensional incompressible fluid (water in these experiments). Even though the underlying fluid is incompressible, the floating particles form a compressible system. If the water molecules should move downward at some point at the surface ($z=0$), the floaters, which cannot follow this downward motion, will accumulate there. Likewise they will flee the upwelling points. Since the underlying flow is assumed to be turbulent, the pattern the floaters form will fluctuate in both time and space. The floaters are chosen to be small enough that they follow the velocity field at the surface; their inertia is negligible (see below). Neglecting the wave motion of the surface (which is negligible), the floaters move in a plane. They are merely sampling the velocity field of the incompressible flow at the surface, and hence their velocity at each instant t is the same as that of the surface water molecules $[v_x(x,y,0,t),v_y(x,y,0,t)]=\mathbf{v}(\mathbf{x},t)]$. The geometrical pattern formed by the floaters has a fractal appearance, as seen in Fig. 2(a), which reaches a statistical steady state in approximately 1s. This work focuses on the geometric and dynamic behavior of the floaters in the steady state.

The coagulation phenomenon studied here and in BDES has nothing to do with the interaction between the floaters or the waves that are present on the surface; all the effects observed in the laboratory are also seen in computer simulations, where these two effects are not included [1,4]. If the flow field is isotropic, one can define a dimensionless compressibility at the surface,

$$\mathcal{C}=\frac{\langle(\partial_x v_x+\partial_y v_y)^2\rangle}{2\langle(\partial_x v_x-\partial_y v_y)^2\rangle}, \tag{1}$$

which lies between 0 (incompressible flow) and 1(potential flow). In the simulations $\mathcal{C}$ is an adjustable parameter, but in the experiments it is measured to be very close to 1/2 [4]. The computer simulations yield a value very close to this [1,4]. In these experiments a descriptor of the coagulation pattern is extracted from the data, namely the "information dimension" D_1, which is defined below. It is simply related to $\mathcal{C}$ in the Kraichnan model [1]. Thus, the measurement of D_1 provides an experimental test of the applicability of the Kraichnan model for temporally decorrelated data.

II. EXPERIMENT

The experiments are carried out in a tank 1 m $\times$ 1 m in lateral dimensions, filled with water to a depth of 30 cm.

*Corresponding author; jml37+@pitt.edu

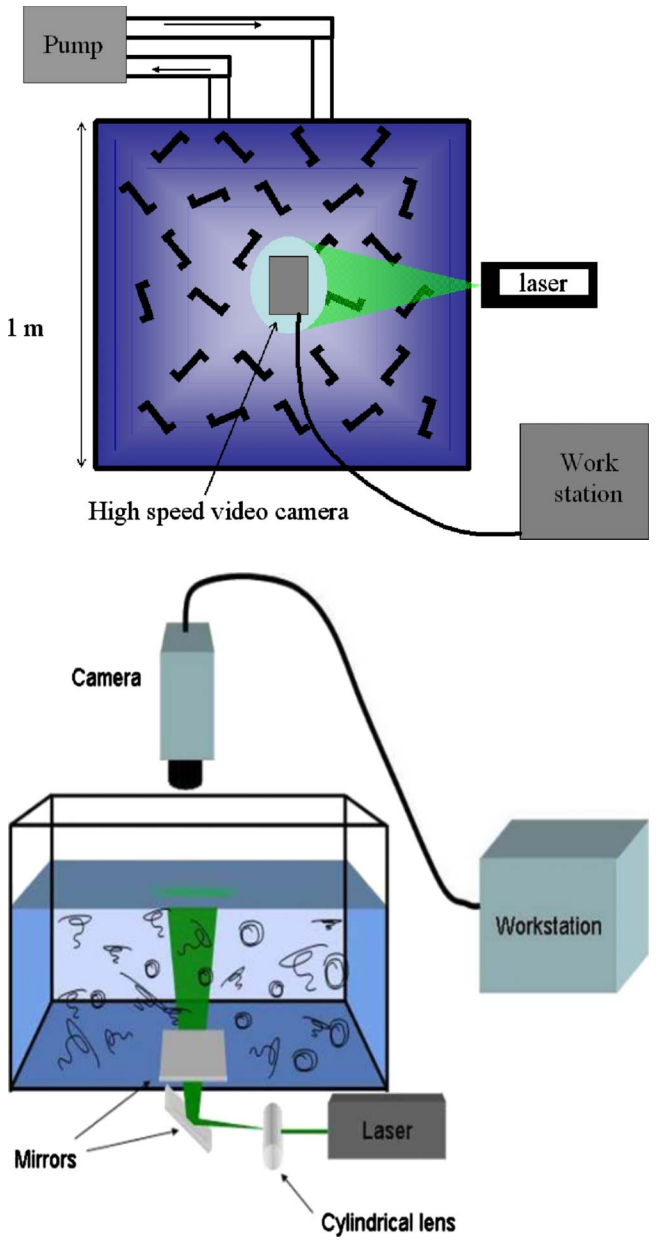

FIG. 1. (Color online) Schematic of the top-view (top panel) and side-view (bottom panel) of the experimental setup. 36 rotating capped jets are placed horizontally on the tank floor (shown as randomly oriented Z-shaped patterns) that pump water into the tank recirculated by a 8hp pump. The central region of the water surface is illuminated by a laser sheet. A high-speed digital camera suspended vertically above this central region captures images of the light scattered by buoyant particles (50 μm hollow-glass spheres of specific gravity 0.25).

Turbulence is generated by a pump ($8hp$) which re-circulates water through a system of 36 rotating jets placed horizontally across the tank floor (see Fig. 1). This system for generating the turbulence ensures that the source of turbulent injection is far removed from the free surface where the measurements are made [4]. More importantly, the method also minimizes the amplitude of surface waves, which are unavoidable. Prior experiments have demonstrated that the waves at the surface have negligible influence on the experimental results [4].

The hydrophilic particles chosen here are subject to capillary forces which are very small compared to forces coming from the turbulence, and do not affect the results as they do in [5,6]. The noninertial character of the particles is minimal because the product $\tau_s\lambda_1$, where λ_1 is the largest Lyapunov exponent and τ_s is the stopping time of the particle [7], is of the order 5×10^{-4}, which is too small to lead to any significant inertial effect [4].

During an experimental run, floating particles (50 μm diameter and specific gravity of 0.25) are constantly seeded into the fluid from the tank floor, where they undergo turbulent mixing as they rise due to buoyancy. Their motion is tracked via a high-speed camera (Phantom v.5) situated above the tank. The camera field-of-view is a square area of side length $L=9$ cm. The constant particle injection is necessary to replace particles at the surface during the experiment. The source and sink structure at the surface fluctuates in both time and space, which can cause particles to leave the camera's field of view. This experimental scheme has been used several times before [4,8], including a detailed comparison of the experiment with numerical simulations.

The instantaneous velocity field of the floaters is measured using an in-house developed particle imaging velocimetry (PIV) program, which processes the recorded images of the surface particles. The constant injection of particles ensures that surface sources and sinks receive an adequate

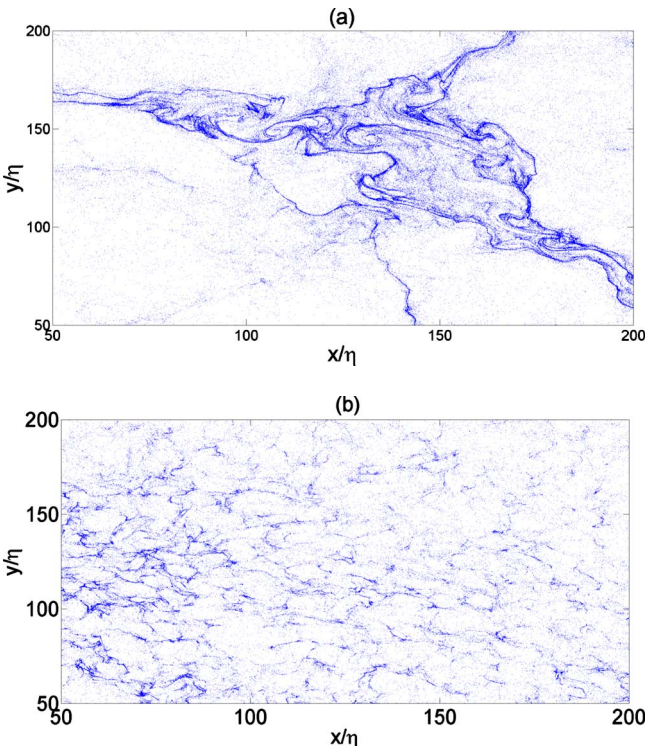

FIG. 2. (Color online) Visualization of particle distributions for the correlated flow (a) and the decorrelated flow (b) at $t/\tau_0=5$. The time scale is in units of the large eddy turnover time τ_0. The initial distribution ($t/\tau_0=0$) is homogeneous with 4×10^5 particles. Both particle distributions are in the steady state. Notice that for the correlated flow, there are coherent structures at large scales ($r>50$). For the decorrelated flow, these large scale structures are not present, but linelike coagulations persist at scale $r<10$.

TABLE I. Turbulent parameters measured at the surface. Measurements are made at several values of the Re_λ with an average $\mathrm{Re}_\lambda \simeq 160$. The parameters listed are averages, with deviations less than 10%.

Taylor microscale	$\lambda = \sqrt{\frac{v_{rms}^2}{\langle(\partial v_x/\partial x)^2\rangle}}$	0.47 (cm)
Taylor Re_λ	$\mathrm{Re}_\lambda = \frac{v_{rms}\lambda}{\nu}$	160
Integral Scale	$l_0 = \int dr \frac{\langle v_\parallel(x+r)v_\parallel(x)\rangle}{\langle(v_\parallel(x))^2\rangle}$	1.42 (cm)
Large Eddy Turnover Time	$\tau_0 = \frac{l_0}{v_{rms}}$	0.43 (s)
Kolmogorov Time	$\tau_\eta = \frac{\nu}{\epsilon}^{1/2}$	0.04 (s)
Dissipation Rate	$\varepsilon_{diss} = 10\nu\langle(\frac{\partial v_x}{\partial x})^2\rangle$	6.05 $(\mathrm{cm}^2/\mathrm{s}^3)$
Kolmogorov scale	$\eta = (\frac{\nu^3}{\varepsilon})^{1/4}$	0.02 (cm)
RMS Velocity	$v_{rms} = \sqrt{\langle v^2\rangle - \langle v\rangle^2}$	3.3 (cm/s)
Compressibility	$\mathcal{C} = \frac{\langle(\vec{\nabla}_2\cdot\vec{v})^2\rangle}{\langle(\vec{\nabla}_2\vec{v})^2\rangle}$	0.49 ± 0.02

coverage on the surface. The local particle density at the surface determines the average spacing of the velocity vector fields produced by the PIV program. The resulting velocity vectors are spaced (on average) by $\delta x = 2.5\eta$ over both sources and sinks, where η is the dissipative scale at the surface (Table I). This density of the vector grid spacing is important for the Lagrangian particle evolution scheme, which is discussed below.

The camera height above the water surface was chosen so that a pixel size is roughly $0.1mm$, comparable to η (see Table I). Data were taken for several values of $\mathrm{Re}_\lambda \simeq 150-170$ (defined in Table I) with an average $\mathrm{Re}_\lambda \simeq 160$. The measurements in this experiment show no systematic variation with the Re_λ over this range, so they are used as an ensemble average so as to decrease measurement errors. Turbulent parameters measured at the surface are listed in Table I. The camera frame rate is set between 100–200 Hz, such that each instantaneous velocity vector field is separated by approximately $4-8\tau_\eta$, where τ_η is the lifetime of eddies of size η (see Table I). Results reported here do not depend on this frame rate.

The experimentally measured velocity fields were then used to solve the equation of motion for Lagrangian particles:

$$\frac{d\mathbf{x}_i}{dt} = \mathbf{v}(\mathbf{x}_i(t), t), \tag{2}$$

where $\mathbf{v}(\mathbf{x}_i, t)$ is the velocity field and $\mathbf{x}_i = (x_i, y_i)$ are the individual particle positions.

To achieve accurate results for the Lagrangian particle evolution, the vector fields used in Eq. (2) were interpolated from the experimentally determined velocity vectors via a bicubic interpolation scheme developed for numerical simulations, as discussed in [9] and implemented in [4]. This scheme uses the smooth flow between grid points separated by length scales comparable to η to interpolate the velocity field between measured grid points. To use this scheme it is necessary for the measured grid spacing to satisfy the criterion $\delta x < \pi\eta$, where δx is the measured velocity grid spacing. We have tested to ensure that the results do not depend on the velocity grid spacing by varying the spacing from $\delta x = 2.5\eta$ to $\delta x = 4\eta$ (increasing this average spacing even further degrades the statistical quality of the data).

For the correlated flow data, a uniform distribution of Lagrangian tracers is generated at time $t/\tau_0 = 0$, where $\tau_0 = \delta U(l_0)/l_0$ is the large eddy turnover time. Here, $\tau_0 = 0.4$ s. The uniform distribution is then evolved using the above-described scheme with the velocity vector field record in the order it was taken during the experiment. To de-correlate the data, we take successive snapshots of the Eulerian velocity field and put them in random order. An initially uniform particle distribution is then evolved from this shuffled record. The velocity vector field record spans roughly 60 τ_0. The results in this work were unaffected when this record was cut in half, suggesting that the data record is long enough to mimic delta correlation in time. Visualizations of the correlated and decorrelated particle distributions (in the steady state) are shown in Figs. 2(a) and 2(b), respectively. The qualitative impression from the two images is that both distributions lie along linelike structures, but for the correlated flow these structures span up to several integral length scales, $l_0/\eta \simeq 70$, where l_0 is defined in Table I.

III. INFORMATION DIMENSION D_1

The information dimension D_1 is measured by dividing the system's field of view into boxes of size $r = s/\eta$, where s is the box size in cm, making r dimensionless. One then calculates the probability $P_i(r)$ of box i being populated. The information dimension D_1 is defined as:

$$D_1 = \lim_{r\to 0} \frac{-I(r)}{\log r}. \tag{3}$$

The function $I(r)$, is called the information function, is defined as

$$I(r) = -\sum_i P_i(r)\ln[P_i(r)]. \tag{4}$$

To calculate D_1, one plots $I(r)$ vs $\log r$. The slope of this line is D_1 over the interval of r where this plot is a straight line. Figure 3 shows $I(r)$ vs $\log r$ of the correlated and decorrelated particle distributions seen in Fig. 2. For the correlated flow, $D_1 = 1.16 \pm 0.02$ and for the decorrelated flow, $D_1 = 1.09 \pm 0.02$, measured over the interval $0.2 < r < 3$. We choose to label this range of r as being in the dissipative range. This is consistent with the fact that the transition from the inertial to dissipative range in many experiments occurs at $r > 1$ [10,11].

The qualitative impression that both distributions lie along linelike structures is consistent with D_1 being close to unity. This finding is consistent with the DNS performed in [1], where it was found that $D_1 = 1.15$ for the correlated flow. At values of $r > 10$ (in the inertial range), the correlated and decorrelated distributions differ significantly. For the correlated flow in Fig. 2(a), the linelike structures extend over several integral length scales l_0. These large-scale structures of the correlated flow give rise to a value of D_1 that is larger than its small-scale value $(0.2 < r < 3)$, as more clearly seen

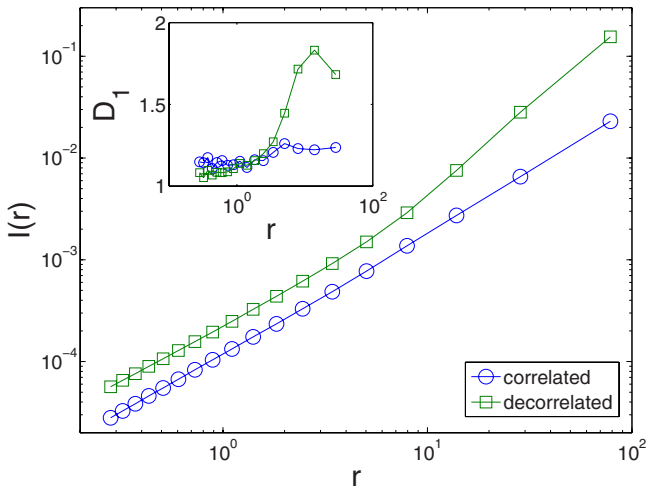

FIG. 3. (Color online) Plot of information function $I(r)$ versus $r=s/\eta$ for the correlated and decorrelated flows at $t/\tau_0=5$. Scale-free behavior is observed for $0.2<r<3$. The inset shows the quality of the scale-free behavior. For the correlated flow $D_1=1.16\pm0.02$, and for the decorrelated flow $D_1=1.09\pm0.02$. The most conspicuous difference between the correlated and decorrelated flows is the lack of scaling in the inertial range for the decorrelated flow. This reflects the loss of large-scale structures when the flow is decorrelated. The prediction for D_1 in the Kraichnan ensemble is $D_1\simeq1$.

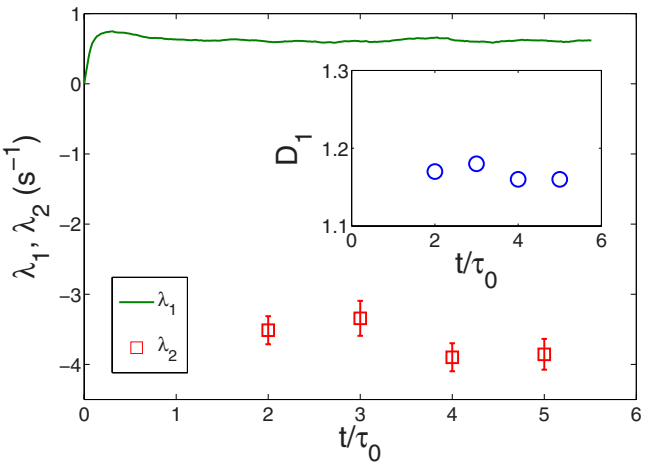

FIG. 4. (Color online) Calculation of the largest Lyapunov exponent λ_1 for the correlated flow. The information dimension D_1 is calculated (inset) at several instants of time once the largest Lyapunov exponent has saturated to a steady-state value of the $\lambda_1=0.6$ Hz. From Eq. (7), one can estimate the value of the second Lyapunov exponent $\lambda_2=-3.5\pm0.26$ Hz from λ_1 and D_1. The sum of the Lyapunov exponents is related to the entropy rate $\dot{S}=\lambda_1+\lambda_2=-2.9\pm0.3$ Hz. This is comparable to the entropy rate $\dot{S}=-2.4\pm0.02$ Hz measured in [8].

in the inset of Fig. 3. This inertial range scaling is consistent with the results of a model for adjustably compressible flow in [12]. For the decorrelated flow, the distribution is more homogeneous over the inertial range, where scale-free behavior is not apparent. This demonstrates (quantitatively) the importance of time correlation for the formation of large-scale coherent structures.

The Kraichnan model of time-decorrelated velocity fluctuations provides a simple relation between the information dimension D_1 and the compressibility $\mathcal{C}$ [1]:

$$D_1=\frac{2}{1+2\mathcal{C}}, \tag{5}$$

both of which are measured in this study. The transition to strongly compressibile flow takes place at $\mathcal{C}=1/2$, which is approximately what is seen in this experiment. For the decorrelated flow in this experiment, $D_1=1.09\pm0.02$, which is measurably greater than unity. The decrease in the dimension D_1 for the decorrelated flow in this experiment is consistent with the results in [1], but the value obtained is larger than the Kraichnan prediction of $D_1\simeq1$.

IV. LYAPUNOV EXPONENTS

The information dimension D_1 was obtained in BDES from a measurement of the two Lyapunov exponents, which have been measured in this experiment as well. The Lyapunov exponents of the floaters give a measure of the mean rate at which particle pairs separate on the surface. In $d=2$ dimensions, the largest is λ_1 (which is positive), and the smallest $\lambda_2<0$. Since the floaters coagulate, their sum is negative. These exponents are defined so that each pair is initially separated by a distance r_0 that is very small (less than η in the turbulent case). Since the Lyapunov exponents define an average rate of separation, a pair must be tracked for a long enough time that their rate of separation has become time independent, but not so long that their final separation has become greater than η [13].

Instead of allowing particle pairs to separate continuously, λ_1 is calculated by the algorithm given in [14]. After each frame, a given particle pair's separation $r(t)$ is reset to r_0 and evolved again. This is done in the limit that $t\to\infty$, where λ_1 should saturate to it's steady-state limiting value. The particle pairs are evolved using the same Lagrangian evolution scheme discussed above. The results presented here do not depend on r_0, which was varied from 0.25η to 1η. An initial separation of $r_0=0.25\eta$ is used. Here, we evolve an ensemble of particle pairs (10^6) for a maximum of $5\tau_0$, which corresponds to roughly $100\tau_\eta$ ($\tau_0=0.4$ s and $\tau_\eta=0.04$ s). The calculation of λ_1 is thus:

$$\lambda_1=\lim_{t\to\infty}\frac{1}{t}\left\langle\log\frac{r(t)}{r_0}\right\rangle, \tag{6}$$

where the angular brackets denote an ensemble average over the various particle pairs. From Figs. 4 and 5 it is seen that after a small transient time (of roughly τ_0), λ_1 saturates to a value of 0.6 Hz (correlated) and 0.5 Hz (decorrelated) (see Table II). Also shown in Figs. 4 and 5 are values of D_1 measured at various times during the experiment after λ_1 has saturated.

One can calculate the value of λ_2, using λ_1 and D_1, from the Kaplan-Yorke relation (which is exact in two dimensions) [15]:

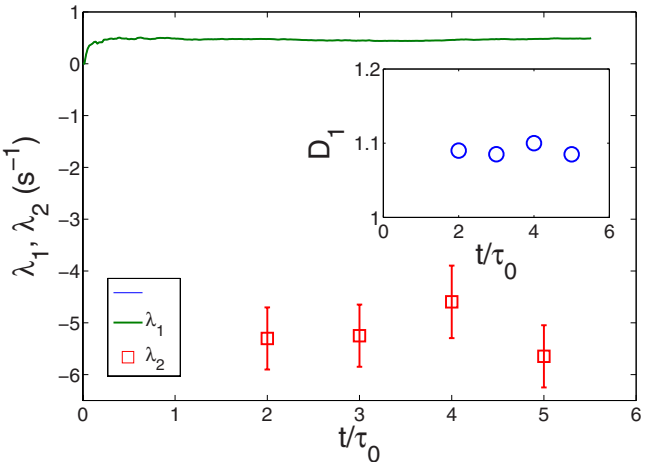

FIG. 5. (Color online) Calculation of the largest Lyapunov exponent λ_1 for the decorrelated flow. The information dimension D_1 is calculated (inset) at several instants of time once the largest Lyapunov exponent has saturated to a steady-state value of the $\lambda_1 = 0.5$ Hz. From Eq. (7), one can estimate the value of the second Lyapunov exponent $\lambda_2 = -5.2 \pm 0.44$ Hz from λ_1 and D_1. The important difference between the correlated and decorrelated flows is not the change in the Lyapunov exponents, but the decrease in the dimension D_1, which is consistent with the results in [1]

$$D_1 = 1 + \lambda_1/|\lambda_2|. \tag{7}$$

From this equation, λ_2 is calculated for both the correlated and decorrelated flows in Figs. 4 and 5, respectively. The results from this experiment and from the simulations in BDES, which are summarized in Table II, confirm what the eye sees in Fig. 2: D_1 is roughly equal to unity (the particles cluster into stringlike clusters), and the sum of the Lyapunov exponents is negative.

There is an additional reason for measuring λ_1 and λ_2; their sum is related to a quantity measured in a prior experiment, providing an additional check on the internal consistency of all the experimental observations. In a prior experiment by Bandi *et al.* [8], the mean rate of change of the entropy of the floaters, $\langle dS/dt \rangle$, was measured in the same tank used in the present experiments, though at a Re_λ of 100 instead of 160. Here S is the entropy, defined as $S = -\Sigma_i P_i \ln(P_i)$, which is Eq. (4) in the limit that the box size r is sufficiently small.

This mean entropy rate $\langle dS/dt \rangle$ is the spatially averaged divergence of the velocity field at the surface [8]. It is also equal to the sum of the Lyaunov exponents, $\langle dS/dt \rangle = \lambda_1 + \lambda_2$, if the turbulent flow is statistically stationary [15]. In [8] $\langle dS/dt \rangle \simeq -2.4$ Hz, while the present experiment gives $\Sigma = -3.15 \pm 0.5$ Hz. In light of the uncertainty in the measurement of the entropy rate in [8], and the difference in Re_λ, this agreement between the two types of measurement of Σ seems quite satisfactory. In comparing the simulation of BDES with these experiments, it should be born in mind that the laboratory results have appreciable uncertainty, while there is no error (or units) quoted for the simulations.

V. SUMMARY

Turbulence is especially difficult to understand because the velocity fluctuations, which lie at its heart, are chaotic in both space and time, with very many degrees of freedom being excited. The phenomenon is especially intractable when viewed in the Eulerian frame, where the small-scale velocity fluctuations are contained in, and moved about, by eddies of larger size.

In an effort to capture the essence of turbulence, R. Kraichnan, and L. F. Richardson before him, proposed that the problem is more easily understood in the Lagrangian frame, where large-scale sweeping effects are absent. To effect further simplification, Kraichnan proposed that the temporal velocity fluctuations be treated as in Brownian motion, i.e., that the correlation time of eddies of all sizes, be approximated as being infinitely short (a Gaussian approximation, as in Brownian motion, is made as well).

This experiment probes a type of compressible flow, namely, the chaotic motion of particles that float on an incompressible and strongly turbulent fluid. The spatiotemporal dynamics of these floaters is studied, and then the observed velocity fluctuations are randomized in time, so as to mimic the simplifying dynamics analyzed by Kraichnan. As predicted, certain aspects of the particle motion and topology are retained in the temporally decorrelated field.

The topology of the decorrelated floaters is stringlike, just as in the correlated case (compare the two panels in Fig. 2). The information dimension D_1 remains close to unity, at least

TABLE II. Parameters measured in this experiment, the simulation of BDES, and a prior experiment where $\langle dS/dt \rangle$ was measured [8].

	D_1	λ_1	λ_2	$\langle dS/dt \rangle$
Experiment				
Correlated	1.16 ± 0.02	0.6 ± 0.05	-3.75 ± 0.26	-3.15 ± 0.5
Decorrelated	1.09 ± 0.02	0.5 ± 0.05	-5.2 ± 0.44	-4.7 ± 0.8
BDES Simulation				
Correlated	1.15			
Decorrelated	1.05			
Bandi Experiment				-2.4 ± 0.02

at small spatial scales where this parameter is defined. On large scales, temporal decorrelation truncates the length of the stringlike structures, as seen in Fig. 2. The present measurements, and those of BDES [1], show that D_1 (and presumably other fractal dimensions) is measurably altered by the temporal randomization, but at small scales the particle distribution retains its string-like character.

The effect of temporal randomization on the two Lyaponuv exponents is more delicate. For both the correlated and decorrelated flows, the positive exponent λ_1 remains positive (patches of particles are stretched into strings in both cases), but decorrelation compacts the structures into thinner strings, i.e., λ_2 is decreases from roughly -3 to -5 Hz.

The steady-state entropy rate of change dS/dt, which for a flow admitting Sinai-Ruelle-Bowen (SRB) statistics is the sum of λ_1 and λ_2 [16,17], is lowered by decorrelation; it becomes even more negative. The measurements reported here, and the simulations of Boffetta *et al.*, suggest that our understanding of turbulence can be enhanced by comparing and contrasting correlated and temporally decorrelated flows.

ACKNOWLEDGMENTS

We acknowledge very helpful discussions with M. M. Bandi, A. Pumir, G. Boffetta, and J. Schumacher. Funding was provided by the U.S. National Science Foundation Grant No. DMR-0604477.

[1] G. Boffetta, J. Davoudi, B. Eckhardt, and J. Schumacher, Phys. Rev. Lett. **93**, 134501 (2004).
[2] R. Kraichnan, Phys. Fluids **11**, 945 (1968).
[3] L. F. Richardson, Proc. R. Soc. London, Ser. A **110**, 709 (1926).
[4] J. R. Cressman, J. Davoudi, W. I. Goldburg, and J. Schumacher, New J. Phys. **6**, 53 (2004).
[5] P. Denissenko, G. Falkovich, and S. Lukaschuk, Phys. Rev. Lett. **97**, 244501 (2006).
[6] G. Falkovich, A. Weinberg, P. Denissenko, and S. Lukaschuk, Nature (London) **435**, 1045 (2005).
[7] M. M. Bandi, J. R. Cressman, and W. I. Goldburg, J. Stat. Phys. **130**, 27 (2008).
[8] M. M. Bandi, W. I. Goldburg, and J. R. Cressman, EPL **76**, 595 (2006).
[9] P. K. Yeung and S. Pope, J. Comput. Phys. **79**, 373 (1988).
[10] C. Meneveau, Phys. Rev. E **54**, 3657 (1996).
[11] R. Benzi, S. Ciliberto, C. Baudet, G. R. Chavarria, and R. Tripiccione, EPL **24**, 275 (1993).
[12] L. Ducasse and A. Pumir, Phys. Rev. E **77**, 066304 (2008).
[13] V. Artale, G. Boffetta, and A. Celani, Phys. Fluids **9**, 3162 (1997).
[14] A. Wolf, J. B. Swift, H. L. Swinney, and J. A. Vastano, Physica D **16**, 285 (1985).
[15] J. R. Dorfman, *An Introduction to Chaos in Nonequilibrium Statistical Mechanics* (Cambridge University Press, Cambirdge, England, 1999).
[16] G. Falkovich and A. Fouxon, New J. Phys. **6**, 50 (2004).
[17] G. Falkovich and A. Fouxon, e-print arXiv:nlin/0312033v1.